

BMAP-28, an Antibiotic Peptide of Innate Immunity, Induces Cell Death through Opening of the Mitochondrial Permeability Transition Pore

Angela Risso,^{1*} Enrico Braidot,² Maria Concetta Sordano,³ Angelo Vianello,² Francesco Macrì,² Barbara Skerlavaj,¹ Margherita Zanetti,¹ Renato Gennaro,⁴ and Paolo Bernardi³

Department of Biotechnology and Biomedical Sciences,¹ and Department of Biology and Agro-Industrial Economics,² University of Udine, I-33100 Udine, C.N.R. Center for the Study of Biomembranes at the Department of Biomedical Sciences, University of Padua, I-35121 Padua,³ and Department of Biochemistry, Biophysics, and Chemistry of Macromolecules, University of Trieste, Trieste,⁴ Italy

Received 22 May 2001/Returned for modification 27 July 2001/Accepted 13 November 2001

BMAP-28, a bovine antimicrobial peptide of the cathelicidin family, induces membrane permeabilization and death in human tumor cell lines and in activated, but not resting, human lymphocytes. In addition, we found that BMAP-28 causes depolarization of the inner mitochondrial membrane in single cells and in isolated mitochondria. The effect of the peptide was synergistic with that of Ca²⁺ and inhibited by cyclosporine, suggesting that depolarization depends on opening of the mitochondrial permeability transition pore. The occurrence of a permeability transition was investigated on the basis of mitochondrial permeabilization to calcein and cytochrome *c* release. We show that BMAP-28 permeabilizes mitochondria to entrapped calcein in a cyclosporine-sensitive manner and that it releases cytochrome *c* in situ. Our results demonstrate that BMAP-28 is an inducer of the mitochondrial permeability transition pore and that its cytotoxic potential depends on its effects on mitochondrial permeability.

Mitochondria are the focus of intense research as major integrators and regulators of cell death pathways (7, 8, 10, 15). Release of death-promoting factors by mitochondria has been reported as a regulatory event in apoptotic death mediated by different signals (20, 35, 37, 39). Mitochondrial dysfunction may also cause necrotic death, and the role played by mitochondria has been well documented in several experimental systems (1, 21, 23, 40). The central role of mitochondria as integrators of the death effector mechanisms is suggested by the fact that several signals derived either from external stimuli or from the cytosol or nucleus converge on mitochondria to trigger cell death (8).

The human antimicrobial peptide hystatin 5 was recently added to the number of toxic agents that act through mitochondria. This molecule is cytotoxic to *Candida albicans* in a manner dependent on functionally active mitochondria, as inhibition of respiration protects the cells from its toxicity (16). Likewise, de-energized human cell lines are protected from the cytotoxic effects of other antimicrobial peptides such as the human defensins (25, 26) and the bovine BMAP-28, a cationic peptide of the cathelicidin family (34, 36, 45). The latter agent causes membrane permeabilization and death of activated human lymphocytes and tumor cells (34). The cytotoxic activity has been related to the structural features of the peptide, which consists of a cationic N-terminal sequence predicted to assume an amphipathic α -helical conformation (residues 1 to 18) and a C-terminal hydrophobic tail (residues 19 to 27). The C-terminal sequence seems to be crucial for the cytotoxic ac-

tivity, as a great reduction of this effect is observed with the synthetic analogue BMAP-28(1-18) comprising the 18 N-terminal residues (36). A second requirement for cytotoxicity is an active metabolism of the target cells, as BMAP-28 is ineffective in nonrespiring cells (34).

In view of these observations, we have investigated whether mitochondria are targets of the peptide itself and/or mediators of its cytotoxic effect. We show that BMAP-28 dramatically affects mitochondrial membrane permeability. Indeed, the peptide caused mitochondrial depolarization, permeabilization to calcein, and in situ cytochrome *c* release. These effects were detected at micromolar or even submicromolar concentrations of the full-length peptide but not detected in BMAP-28(1-18), were potentiated by Ca²⁺ ions, and were inhibited by cyclosporine (CsA), an inhibitor of the mitochondrial permeability transition pore (PTP) (4, 28). We conclude that perturbation of mitochondrial function and cytochrome *c* release are key events in the cytotoxicity of BMAP-28.

MATERIALS AND METHODS

Cell culture and reagents. The U937 (promonocytic) and K562 (erythroid) cell lines were obtained from the American Type Culture Collection (Rockville, Md.) and were cultured in RPMI 1640 culture medium (Gibco Life Technologies, Paisley, United Kingdom) supplemented with 10% fetal calf serum (FCS) (Gibco), 50 IU of penicillin/ml, 50 μ g of streptomycin/ml, and 2 mM L-glutamine (Gibco). The cell lines were periodically tested for mycoplasma contamination.

Mononuclear cells were isolated by Ficoll-Hypaque (Pharmacia Biotech, Uppsala, Sweden) density gradient centrifugation from peripheral blood of healthy donors. The cells were resuspended in RPMI 1640 medium supplemented with 10% FCS, 50 IU of penicillin/ml, 50 μ g of streptomycin/ml, and 2 mM L-glutamine and were activated with 10 μ g of phytohemagglutinin-P (PHA-P)/ml. After 2 days of culture in 25-cm² cell culture flasks at 37°C in a CO₂ incubator, the blasts were washed and seeded in 24-well plates at 6 \times 10⁵ cells/ml in culture medium containing 100 U of human recombinant interleukin-2 (hrIL-2; Gen-

* Corresponding author. Present address: Department of Biology and Agro-Industrial Economics, University of Udine, via Cotonificio 108, I-33100 Udine, Italy. Phone: 39 0432 558789. Fax: 39 0432 558784. E-mail: angela.risso@dbea.uniud.it.

zyme, Cambridge, Mass./ml, and autologous adherent leukocytes were used as feeder cells.

Unless otherwise specified, all reagents and chemicals were from Sigma (St. Louis, Mo.). Safranin O, JC-1 (5,5',6,6'-tetrachloro-1,1',3,3'-tetraethyl-benzimidazolcarbocyanine iodide), BAPTA-AM [1,2-bis (2-aminophenoxy) ethane-*N,N,N',N'*-tetraacetic acetoxymethyl ester], and calcein-AM were purchased from Molecular Probes (Eugene, Oreg.), dissolved, and stored according to the manufacturer's instructions. 9-Fluorenylmethoxy carbonyl, amino acids, and reagents for peptide synthesis were obtained from PerSeptive Biosystems (Framingham, Mass.) and Novabiochem (Laufelfingen, Switzerland). Reagents for high-performance liquid chromatography purification of the peptides were from LabScan (Dublin, Ireland).

Peptide synthesis and purification. BMAP-28, a 28-residue peptide whose C-terminal glycine is removed to give a 27-residue amidated peptide (36), was synthesized as a C-terminal amide of 27 amino acids (GGLRSLGRKILRAWK KYGPIIVPIIRI-am). Solid-phase synthesis of this molecule, of the analogue BMAP-28(1-18) (GGLRSLGRKILRAWKKYG-am), and of the fragment corresponding to the fibronectin region (CS-5) (GEEIQIGHIPREDVDYHLYP) was carried out on a Milligen 9050 synthesizer (Bedford, Mass.). After cleavage from the resin, the peptides were purified by reverse-phase high-performance liquid chromatography on a C_{18} Delta-pack column (Waters, Bedford, Mass.). Analytical assays and determination of the concentration were performed as described in reference 36.

Determinations of changes of mitochondrial membrane potential in intact cells. U937 cells in complete medium (2×10^6 cells/ml) were stained with $5 \mu\text{M}$ JC-1 for 20 min at room temperature in the dark (9, 12), then washed in ice-cold phosphate-buffered saline solution (PBS), and incubated at a cell density of 4×10^6 cells/ml for 15 min at 37°C in PBS-5 mM glucose with the peptides or with FCCP [carbonylcyanide-*p*-(trifluoromethoxy)phenylhydrazone] for 45 min. Cells were analyzed immediately with a flow cytometer equipped with the Cell Quest software by using a 488-nm argon ion laser as the excitation source (FACScan; Becton Dickinson, Mansfield, Mass.). In a parallel experiment, the cells were treated with the peptides as described above and then stained with propidium iodide ($10 \mu\text{g/ml}$) and analyzed with the cytofluorimeter. The same procedure was used for K562 cells and activated lymphocytes, with the exception that the treatment of lymphocytes with BMAP-28 or FCCP was carried out in RPMI-10% FCS.

When indicated, $10 \mu\text{M}$ BAPTA-AM was added to the cell suspensions throughout the staining with JC-1 and the incubation with the peptides. In the experiments with CsA, the cells were stained with JC-1 as described above, then incubated with $10 \mu\text{M}$ CsA for 40 min at 37°C in RPMI-10% FCS, washed in PBS, and treated with BMAP-28 or with FCCP in the presence of CsA.

After 30 min of incubation, the peptide caused necrotic death and disruption of 30 to 35% of the cells, as determined by cytofluorimetric analysis of physical parameters (forward and side light scattering) and lactate dehydrogenase release assay of the cell culture supernatants (34). We therefore monitored the changes in $\Delta\Psi_m$ after a shorter incubation time (15 min), and we gated out dead cells and debris (25 to 30% of all cells) by analyzing the cells stained with propidium iodide on FSC (forward scatter) versus FL3 (propidium fluorescence). A gate set on the FSC-FL3 dot plot for each sample was used to include only viable cells in the analysis of the parallel cell population stained with JC-1. Cells (10,000 per sample) were examined on an FL-1 (530 nm) versus FL-2 (585 nm) dot plot, and the data were analyzed with the Cell Quest software.

The functional assay for multidrug resistance pumps in U937 cells was performed by using the probe rhodamine 123 as described in references 2 and 43. Briefly, cells (5×10^5 cells/ml) were stained with $0.1 \mu\text{M}$ rhodamine 123 for 15 min at 37°C in complete medium, then were centrifuged, resuspended in rhodamine-free medium, and cultured at 37°C . At the indicated time points, 5×10^5 cells were analyzed by flow cytometry.

Preparation of mitochondria and measurement of the membrane potential. Mouse liver mitochondria from male BALB/c mice (6 to 8 weeks old) were isolated by standard centrifugation techniques. All of the steps were carried out at 4°C . Briefly, mouse livers, placed in ice-cold homogenization solution (250 mM sucrose, 1 mM EGTA, 5 mM Tris-HEPES, pH 7.4), were chopped into small pieces and transferred to a precooled glass Potter-Elvehjem homogenizer containing cold homogenization medium. After homogenization, the suspension was filtered through two gauze layers and centrifuged at $1,000 \times g$ for 10 min at 4°C . The supernatant was centrifuged at $10,000 \times g$ for 10 min at 4°C , and the mitochondrial pellet was resuspended in homogenization solution, centrifuged once more, and finally resuspended in 1 ml of suspension buffer (250 mM sucrose, 0.1% fatty acid-free bovine serum albumin [BSA], 5 mM Tris-HEPES, pH 7.4) and kept on ice. The mitochondrial protein was determined by means of the Bradford reagent.

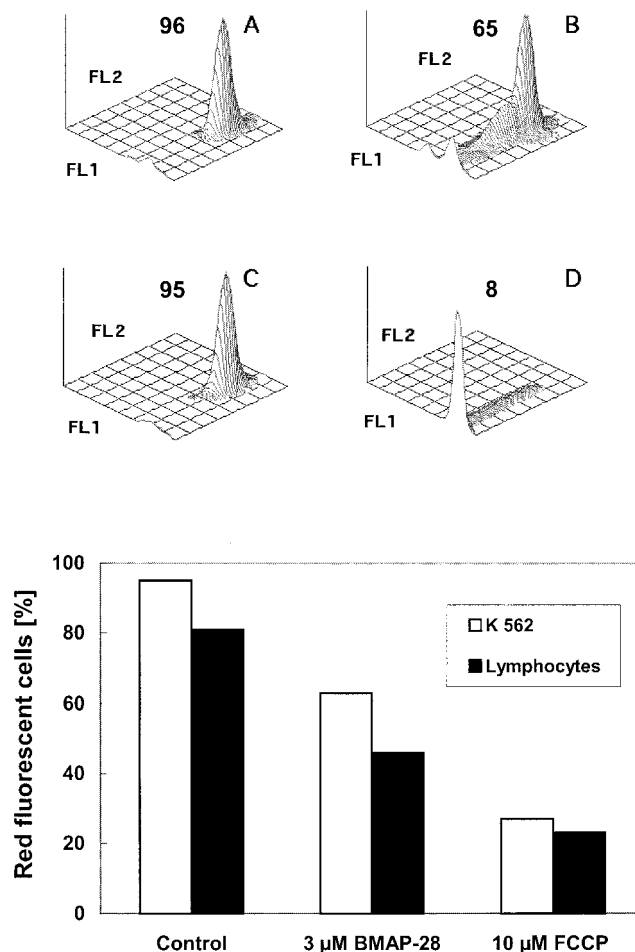


FIG. 1. BMAP-28-induced decrease of mitochondrial membrane potential in situ. Cytofluorimetric analysis and three-dimensional representation of U937 cells stained with $5 \mu\text{M}$ JC-1 and incubated in PBS-5 mM glucose are shown in the upper panel. (A) The CS-5 fragment of fibronectin at a $3 \mu\text{M}$ concentration; (B) $3 \mu\text{M}$ BMAP-28; (C) $3 \mu\text{M}$ BMAP-28(1-18); (D) $10 \mu\text{M}$ FCCP. FL1 (green fluorescence) and FL2 (red fluorescence) are represented in the abscissas and ordinates of the plots, respectively (arbitrary units, 4 log decade scale). The distribution of the cells in the green and red fluorescence channels is represented by the z axis. The figures close to each panel indicate the percentage of the cell population positive for green and red fluorescence assessed by setting a gate on the control cell population, where the majority of the cells had green and red fluorescence intensities above 400 and 120 channels, respectively. One representative experiment out of six is shown. The effects of BMAP-28 on $\Delta\Psi_m$ in K562 cells and in activated human lymphocytes are shown in the lower panel. K562 cells were loaded with JC-1 and then treated with $3 \mu\text{M}$ CsA, BMAP-28, or $10 \mu\text{M}$ FCCP as described above. Lymphocytes from normal human peripheral blood after 8 days of in vitro activation with PHA-P and hrIL-2 were loaded with JC-1 and then incubated with the peptides or FCCP and examined with the cytofluorimeter as described in Materials and Methods. Bars represent the percentage of red fluorescent cells exposed to the indicated treatments, and data are from one representative experiment out of two.

To evaluate $\Delta\Psi_m$ changes, mitochondria were added at a final concentration of 0.1 mg/ml to the assay buffer (250 mM sucrose, 5 mM Tris-HEPES [pH 7.4], 0.1% BSA, 5 mM MgCl_2 , 2 mM KPi , and $5 \mu\text{M}$ safranin O), and fluorescence changes were measured with a Perkin-Elmer spectrofluorimeter (model LS 50 B). The excitation and emission wavelengths were 495 and 586 nm, respectively, with a 10-nm slit width for both emission and excitation (42). Unless otherwise

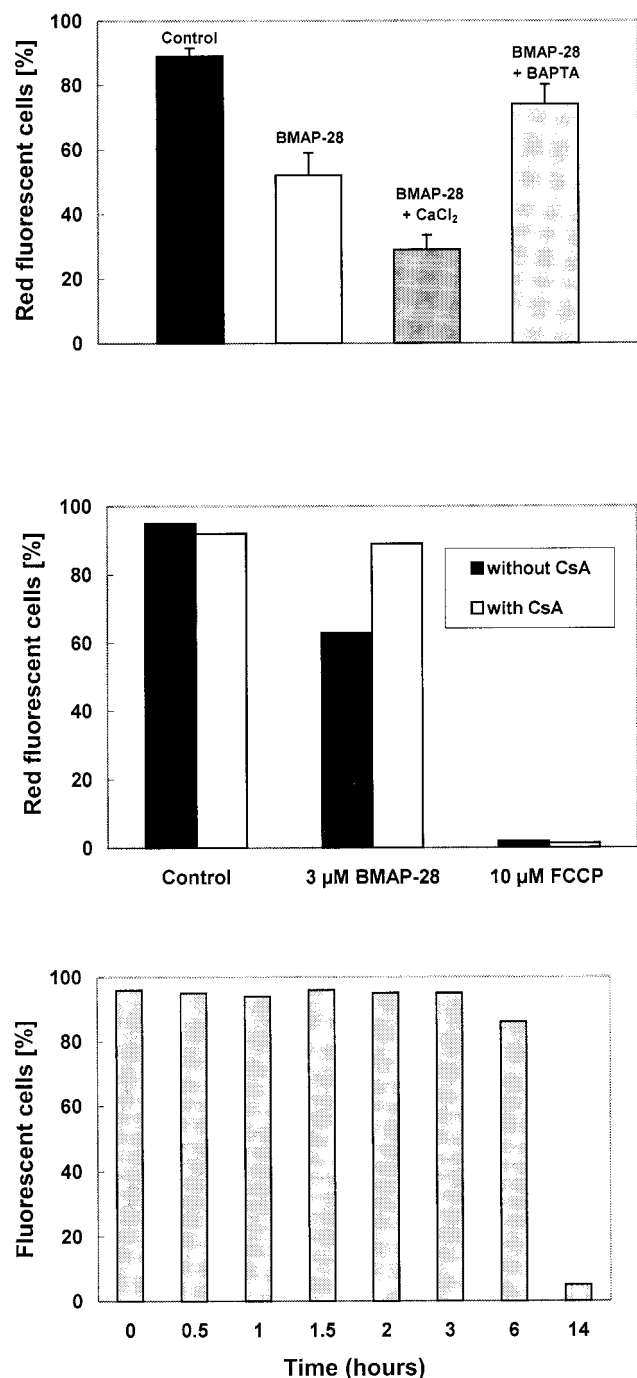


FIG. 2. Effect of Ca^{2+} and CsA on BMAP-28-induced decrease of mitochondrial membrane potential in situ and rhodamine efflux analysis. Results are shown in the top panel for U937 cells preincubated with or without 5 μM BAPTA-AM and stained with JC-1 as described in the legend to Fig. 1 that were treated for 15 min with the 3 μM CS-5 control peptide or with 3 μM BMAP-28 in PBS-5 mM glucose with or without the addition of 2 mM CaCl_2 . The percentage of cells positive for red fluorescence was then assessed by cytofluorimetric analysis. Closed bar, CS-5 peptide; open bar, 3 μM BMAP-28 with no Ca^{2+} added; dark shaded bar, 3 μM BMAP-28 with Ca^{2+} added; light shaded bar, 3 μM BMAP-28 plus BAPTA-AM. The mean values \pm SD of three independent experiments are shown. The middle panel shows results for U937 cells (after loading with JC-1) that were incubated for 40 min at 37°C with 10 μM CsA or with vehicle and then treated with 3 μM BMAP-28 with 10 μM FCCP or with no agent for 15 min at

specified, incubations were carried out at 25°C in the presence of 5 mM succinate as the respiratory substrate. When indicated, 100 μM EGTA was added to the suspension and to the assay buffers to ensure chelation of contaminant Ca^{2+} . CsA was dissolved in ethanol and added to the mitochondria 5 min prior to the addition of other reagents.

The Ca^{2+} concentrations in the assay and suspension buffers containing mitochondria were 100 to 700 nM, as estimated with the Ca^{2+} calibration buffer kit (Molecular Probes) based on the relationship of Ca^{2+} levels to the fura-2 fluorescence intensity ratios at 340 and 380 nm.

Calcein release from mitochondria and intact cells. Mitochondria isolated from mouse livers were incubated at 25°C for 30 min in suspension buffer containing 2 μM calcein AM and then washed and resuspended in the same buffer (31). To assess calcein release, mitochondria (0.1 mg/ml) were added to the assay buffer (250 mM sucrose, 0.1% BSA, 10 μM CoCl_2 , 5 mM Tris-HEPES, pH 7.4) and fluorescence variations were measured with the spectrofluorimeter. The excitation and emission wavelengths were 488 and 515 nm, respectively, with a 5-nm slit width for both emission and excitation. Note that the assay buffer contained 10 μM CoCl_2 to quench the fluorescence of calcein released from mitochondria.

To investigate mitochondrial permeabilization to calcein in intact cells (31), U937 cells were incubated at 37°C for 15 min in Hanks' buffered salt solution with 2 μM calcein-AM and 0.5 mM CoCl_2 , then washed with PBS, and resuspended in PBS-5 mM glucose supplemented with 3 μM BMAP-28 for 10 min at 37°C in the dark. When indicated, after the incubation with calcein-AM, the cells were washed and treated with 10 μM CsA for 40 min at 37°C and then incubated with the peptide. To verify that calcein localized to the mitochondria, calcein loading of the cells was followed by exposure to 0.1 μM tetramethyl-rhodamine methyl ester (TMRM) and the cells were examined with a Zeiss axioplan 2 epifluorescence microscope equipped with a photcamera and an image analyzer with the following filter settings: calcein, 450 to 490 nm excitation and 515 to 565 nm emission; and TMRM, 546 \pm 12 nm excitation and 590 nm emission (31). The cells showing an intact morphology, as assessed by inspection under visible light in phase contrast, were examined under the xenon light source to detect green and red fluorescence. The emissions were collected simultaneously, resulting in a green-orange punctate fluorescence. The green and red components of the images were then analyzed separately (see Fig. 7). Calcein-AM-loaded cells were also analyzed with the cytofluorimeter, gating out dead cells and debris as described above.

Cytochrome *c* release in situ. In situ cytochrome *c* release was studied as described in detail in reference 30. Briefly, cells were incubated with BMAP-28 in PBS-5 mM glucose, then washed with the same medium, spun down onto slides, and fixed for 30 min at room temperature with 3.7% (vol/vol) ice-cold formaldehyde. Following permeabilization for 20 min with 0.01% (vol/vol) ice-cold Nonidet P-40, incubation was continued for 15 min with a 0.5% solution of BSA and then for 15 min at 37°C with the anti-cytochrome *c* antibody and with an affinity-purified rabbit antibody against the rat *bc₁* complex (a generous gift of Roberto Bisson, Padua, Italy). Cells were then sequentially incubated for 15 min at 37°C with tetramethyl rhodamine isothiocyanate-conjugated goat anti-mouse immunoglobulin G and with fluorescein isothiocyanate-conjugated goat anti-rabbit immunoglobulin G. For cytochrome *c* and *bc₁* complex detection, red and green channel images were acquired simultaneously by using two separate color channels on the detector assembly of a Nikon Eclipse E600 microscope equipped with a Bio-Rad MRC-1024 laser scanning confocal imaging system, 488 nm excitation and 522 \pm 25 nm emission band-pass and 568 nm excitation and 605 nm emission long-pass filter settings, and a 60 \times , 1.4 numerical aperture oil immersion objective (Nikon). Twenty randomly chosen fields in each slide were stored for subsequent analysis, which was carried out exactly as described in reference 30. The localization index, computed on a single-cell basis, is defined as the ratio of the standard deviation (SD) of the fluorescence intensity divided by the total fluorescence (Σ) for each channel: $(\text{SD}/\Sigma)_{\text{red}}/(\text{SD}/\Sigma)_{\text{green}}$. A punctate (i.e., mitochondrial) distribution results in a higher SD, while normalization allows correction for different fluorescence intensities in the two channels. A localization index of 1 indicates that cytochrome *c* and the *bc₁* complex have the

37°C, as indicated. The bars represent the percentages of cells positive for red fluorescence. One experiment representative of three separate assays is shown. The lower panel shows results for U937 cells that were incubated with rhodamine 123 as described in Materials and Methods, washed, and incubated in rhodamine-free culture medium for 14 h. At the indicated times, samples of the cell population were analyzed by flow cytometry. One experiment out of three separate assays is shown.

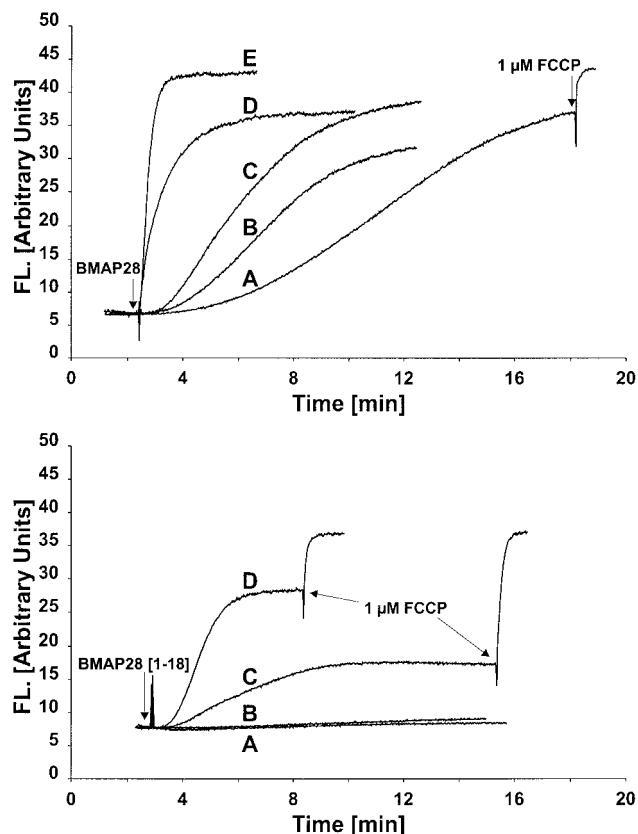


FIG. 3. Effects of BMAP-28 and BMAP-28(1-18) on the mitochondrial membrane potential of mouse liver mitochondria. Mitochondria (0.1 mg/ml) were incubated in 250 mM sucrose, 5 mM Tris-HEPES (pH 7.4), 0.1% BSA, 2 mM P_i , 5 mM $MgCl_2$, and 5 μM safranin O at 25°C, and the fluorescence emission was determined as described in Materials and Methods. After 3 to 5 min, 5 mM succinate was added. When the fluorescence emission was constant, the peptide BMAP-28 or the analogue BMAP-28(1-18) was added (arrows). The upper panel shows results for the addition of BMAP-28 at 100 nM (A), 250 nM (B), 500 nM (C), 2 μM (D), and 3 μM (E). In trace A, further $\Delta\Psi_m$ loss caused by the addition of 1 μM FCCP is shown. The lower panel shows results for the addition of BMAP-28(1-18) at 500 nM (A), 1 μM (B), 2 μM (C), and 3 μM (D). In traces C and D, the effects of the addition of 1 μM FCCP are also shown. A representative experiment out of three is shown.

same distribution, which is expected in normal cells, while an index lower than 1 means that the distribution of cytochrome *c* is more homogeneous than that of the *bc₁* complex. For further details, see reference 30.

Analysis of DNA fragmentation. To assess nuclear degradation, after 15 min of treatment with BMAP-28, U937 cells were incubated in peptide-free culture medium for 18 h. DNA fragmentation was analyzed at 6 and 18 h by agarose gel electrophoresis as described in reference 34. Briefly, cells were lysed with 0.5% Sarkosyl in 50 mM Tris-HCl and 10 mM EDTA (pH 8.0) in the presence of 0.5 mg of proteinase K/ml. After 1 h of incubation at 50°C, RNase A (0.15 mg/ml) was added to each sample. The lysates were analyzed by electrophoresis on 1.2% agarose gels containing 0.5 μg of ethidium bromide/ml.

RESULTS

Effects of BMAP-28 on mitochondrial membrane potential in situ. In order to investigate possible variations of mitochondrial membrane potential ($\Delta\Psi_m$) caused by BMAP-28, we used the U937 cell line, which proved to be one of the most suscep-

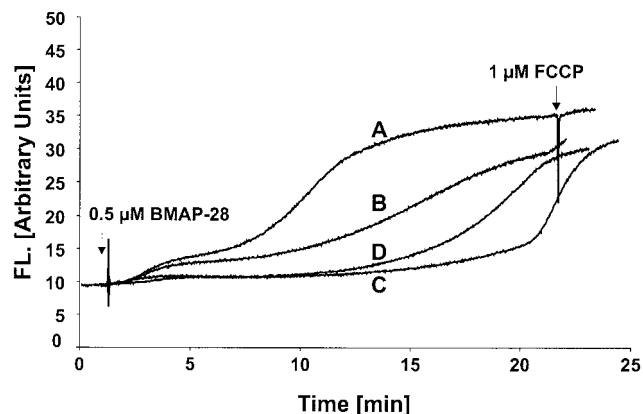


FIG. 4. Effects of CsA on BMAP-28-dependent mitochondrial depolarization. Mitochondria (0.1 mg/ml) were incubated as described in the legend to Fig. 3, and BMAP-28 was added where indicated at a concentration of 500 nM. CsA was absent (A) or present in the incubation mixture from the beginning of the assay at 50 nM (B), 75 nM (C), and 100 nM (D), respectively. Results representative of three separate experiments are shown.

tible targets of peptide cytotoxicity (34). U937 cells were loaded with the potentiometric probe JC-1, and changes of $\Delta\Psi_m$ were evaluated by the shift from the red and green to green fluorescence emission after treatment with 3 μM BMAP-28 for 15 min. The short time of incubation with the peptide enabled us to analyze a cell population where the majority of the cells (65 to 75%, compared to untreated cells) were viable, as shown by the parallel analysis of physical parameters and determination of propidium iodide uptake. The results illustrated in Fig. 1, upper panel, show that cells treated with the fibronectin peptide CS-5 (used here as a negative control) were positive for both red (FL2) and green (FL1) fluorescence (Fig. 1, plot A) while a remarkable decline in the red fluorescence was observed after a 15-min incubation with 3 μM BMAP-28 (Fig. 1, plot B). No fluorescence variation was detectable when 3 μM BMAP-28(1-18), the analogue peptide lacking the hydrophobic sequence (residues 19 to 27), was used (Fig. 1, plot C) while the expected, dramatic decrease of FL2 fluorescent cells followed the treatment with the protonophore FCCP, used as a positive control (Fig. 1, plot D). Similar results were obtained when K562 cells were used as the target cells (Fig. 1, lower panel). We extended our analysis to normal human lymphocytes, which become sensitive to microbicidal doses of BMAP-28 upon in vitro activation (34). After activation by PHA-P and hrIL-2 for 8 days, the lymphoblasts were loaded with JC-1 and treated with CS-5, BMAP-28, or FCCP as described above for U937 cells. As shown in Fig. 1, lower panel, BMAP-28 and FCCP induced a decrease in the percentage of red fluorescent cells. Taken together, these data indicate that BMAP-28 induces an early decrease of mitochondrial membrane potential in both transformed and normal cells and that this event precedes cell death (see below).

In a detailed study of the effects of BMAP-28 on U937 cells, we observed that the percentage of cells showing a decline of the red fluorescence after incubation with BMAP-28 was increased by adding 2 mM Ca^{2+} to the incubation buffer and was lowered by loading the cells with BAPTA-AM, a Ca^{2+} chelator

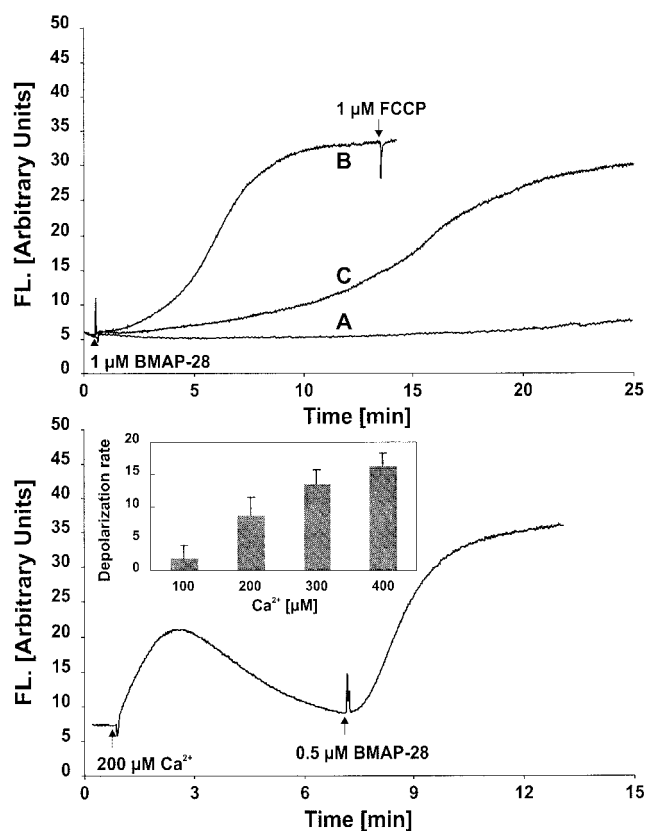


FIG. 5. Effect of Ca^{2+} on BMAP-28-dependent mitochondrial depolarization. Mitochondria (0.1 mg/ml) were incubated as described in the legend to Fig. 3, except that 100 μM EGTA was present in both the suspension buffer and the assay buffer as described in Materials and Methods. The upper panel shows results for BMAP-28 at concentrations of 500 nM (A) and 1 μM (B). Trace C shows results for 1 μM BMAP-28 and 1 μM CsA that was present in the assay medium from the beginning of the incubation. After the addition of 5 mM succinate, different concentrations of CaCl_2 and then 500 nM BMAP-28 were added (lower panel). The trace depicts the transient depolarization caused by Ca^{2+} uptake and the subsequent $\Delta\Psi_m$ decrease mediated by BMAP-28 addition. The inset shows the rate of depolarization by BMAP-28 as a function of the Ca^{2+} concentration as determined from the mean rate of fluorescence emission increase computed in the steepest portion of the traces by the Win Lab software (Perkin-Elmer). The data from a representative experiment out of three are shown.

(Fig. 2, top panel). Furthermore, when the cells were pre-treated with 10 μM CsA, an inhibitor of the PTP, the effect of BMAP-28 was remarkably reduced while, as expected, FCCP was still effective (Fig. 2, middle panel). It should be noted that the activity of the multidrug-resistant P glycoprotein is very low in U937 cells, according to Bailly et al. (2) and our own experiments based on rhodamine 123 efflux (Fig. 2, bottom panel). Thus, the effects of CsA on probe retention by mitochondria cannot be explained by inhibition of the multidrug-resistant pumps by CsA (7).

Since the mitochondrial depolarization induced by BMAP-28 was favored by Ca^{2+} ions, which are physiological effectors of the mitochondrial permeability transition (3, 4), and inhibited by the PTP inhibitor CsA, we further tested whether the cytotoxic effects of BMAP-28 were due, directly or indirectly, to opening the mitochondrial PTP.

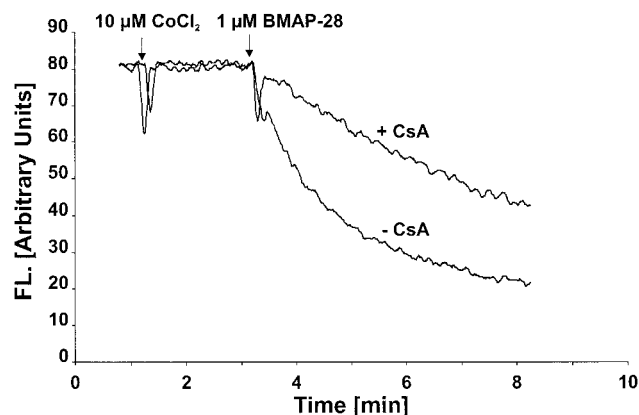


FIG. 6. Effect of BMAP-28 on calcein release from mitochondria. The fluorescence of mitochondria loaded with 2 μM calcein-AM was recorded as described in Materials and Methods. When the emission fluorescence by mitochondria was stable, 10 μM CoCl_2 and 1 μM BMAP-28 were added. When indicated, 1 μM CsA was added to the mitochondrial suspension from the beginning of the assay. A typical experiment out of three is shown.

Effects of BMAP-28 on isolated mitochondria. To evaluate whether BMAP-28 affected mitochondrial function directly, $\Delta\Psi_m$ variations were followed as fluorescence changes of mitochondrial suspensions in the presence of safranin O. The addition of succinate caused a fast quenching of probe fluorescence, due to safranin O uptake by the mitochondria (46). The probe was released by the addition of BMAP-28, and the release rate increased with the concentration of the peptide (Fig. 3, upper panel). It should be noted that the effect was obtained at peptide concentrations between 0.25 and 0.5 μM (2.5 to 5 nmol of mitochondrial protein/mg), which are significantly lower than those required to observe a cytotoxic response (3 to 6 μM) (34). At concentrations of 2 to 3 μM , the peptide caused complete dissipation of $\Delta\Psi_m$ within a few seconds (Fig. 3, upper panel). BMAP-28(1-18), the truncated analogue, proved to be ineffective at concentrations up to 1 μM (Fig. 3, lower panel), and even with higher peptide concentrations, depolarization was only partial (Fig. 3, lower panel).

The mitochondrial depolarization caused by BMAP-28 could be due to a direct effect of the peptide or to activation of an endogenous conductance. In order to assess the possible contribution on the voltage-gated PTP (5) to membrane permeabilization by BMAP-28, we tested the effects of CsA and Ca^{2+} ions. As shown in Fig. 4, CsA was able to significantly delay the depolarization caused by 0.5 μM BMAP-28. On the other hand, the depolarization caused by micromolar doses of both native and truncated peptides was insensitive to CsA (data not shown).

In order to study a possible synergistic effect of Ca^{2+} on BMAP-28-induced depolarization, we resuspended the organelles in assay buffer containing 100 μM EGTA and then we added Ca^{2+} at different concentrations to the incubation mixture before the addition of BMAP-28. In the absence of Ca^{2+} , depolarization required a higher concentration of peptide (1 μM), and under these conditions the effect of the peptide was prevented by 1 μM CsA (Fig. 5, upper panel). When 200 μM

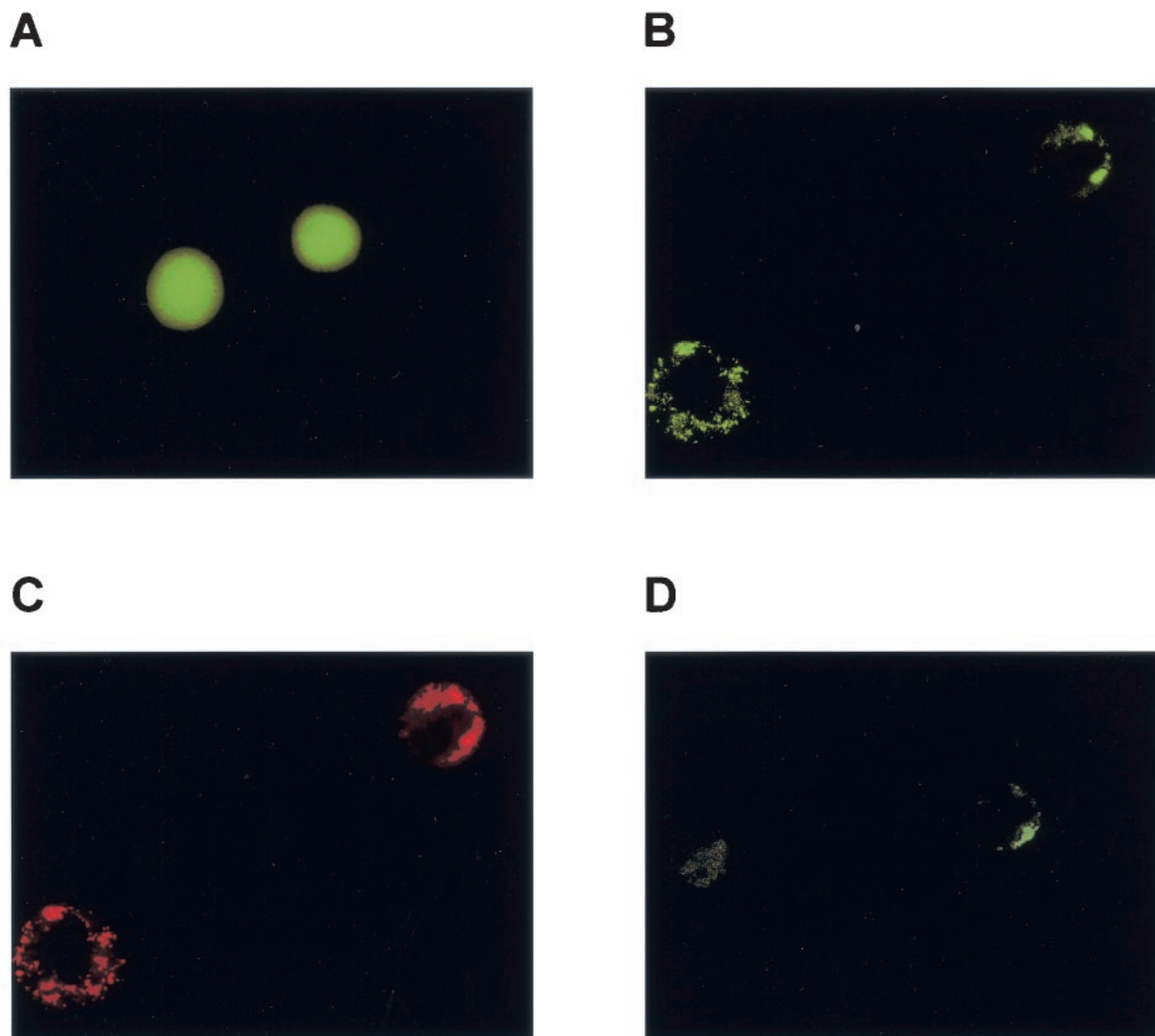


FIG. 7. Effect of BMAP-28 on mitochondrial calcein fluorescence in situ. U937 cells loaded with calcein-AM were analyzed under the epifluorescence microscope as described in Materials and Methods. The cells were stained with 2 μM calcein-AM alone (A) or coloaded with 2 μM calcein-AM and 0.5 mM CoCl_2 (B) followed by 0.1 μM TMRM (C). In panel D, cells loaded with calcein and CoCl_2 (as in panel B) were washed and then treated with 3 μM BMAP-28 for 10 min at 37°C. Only a few fluorescent spots, and some of them very dim, are detectable in cells treated with the peptide.

Ca^{2+} was added, BMAP-28 was again effective at a submicromolar concentration (0.5 μM), as shown by fast safranin dequenching (Fig. 5, lower panel). This effect was further enhanced by adding Ca^{2+} at higher concentrations (Fig. 5, lower panel, inset).

We next studied whether BMAP-28 was able to induce permeation of solutes with a relatively low molecular mass. We loaded mitochondria with the membrane-permeable calcein-AM, which is rapidly converted to the fluorescent calcein (molecular mass, 622 Da) by mitochondrial esterases, and we then resuspended the organelles in an isosmotic medium in the presence of 10 μM CoCl_2 . Since fluorescence emission by calcein is quenched by external Co^{2+} (31), this method allows us to monitor calcein release from mitochondria as the fluorescence decrease of the organelles. Calcein-loaded mitochondria were treated with the peptide, and Fig. 6 shows that a fast

decrease of mitochondrial fluorescence followed the addition of 1 μM BMAP-28. This fluorescence decrease was due to the PTP opening because it was reduced in both rate and extent when CsA was present in the mitochondrial suspensions. A slower, CsA-sensitive decrease of calcein fluorescence was observed at lower concentrations of the BMAP-28 peptide (results not shown).

Effects of BMAP-28 on PTP opening in situ. It is possible to monitor openings of PTP in intact cells by changes in mitochondrial calcein fluorescence after quenching of the cytosolic signal with Co^{2+} (31). To unequivocally test the occurrence of PTP openings as a consequence of BMAP-28 addition to intact cells, U937 cells were treated with calcein-AM, which resulted in cellular loading as demonstrated by a bright, diffuse fluorescence (Fig. 7A). As expected (31), cells coloaded with calcein-AM and CoCl_2 instead displayed a punctate fluorescence

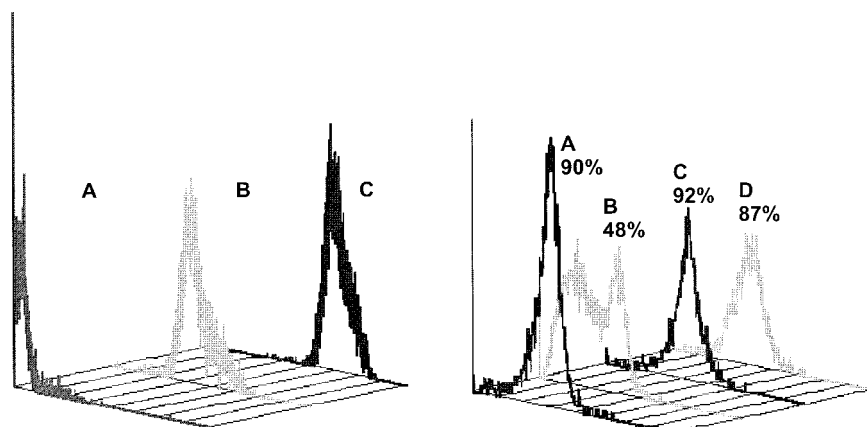


FIG. 8. Cytofluorimetric analysis of the effect of BMAP-28 on mitochondrial calcein fluorescence in situ. Cytofluorimetric analyses of control cells not loaded with calcein-AM (A) and of cells loaded with 2 μ M calcein-AM and 0.5 mM CoCl_2 (B) or with 2 μ M calcein-AM alone (C) are shown in the left panel. Note that after treatment with CoCl_2 , the peak channel of FL1 (green fluorescence) intensity was eightfold lower than that of cells labeled with calcein-AM alone. The right panel shows results for U937 cells loaded with 2 μ M calcein-AM and 0.5 mM CoCl_2 (A) that were incubated with 3 μ M BMAP-28 alone (B) or in the presence of 10 μ M CsA (D). Histogram C shows the profile of cells treated with CsA alone. The histograms are derived from the analysis of viable cells as described in Materials and Methods. The percentage given with each histogram indicates the percentage of cells with an intermediate green fluorescence (as in histogram B in the left panel). In histogram B in the right panel, the peak of negative or dim cells indicates the very low fluorescence of the cells where calcein, released from mitochondria into the cytosol, was quenched by CoCl_2 . Results representative of three separate experiments are shown.

pattern, which is consistent with a mitochondrial distribution (Fig. 7B) as confirmed by the colocalization of TMRM (Fig. 7C). These events were detectable in the cytofluorimetric analysis since the fluorescence intensity of U937 cells loaded with calcein-AM in the presence of CoCl_2 was about eightfold lower than that of cells loaded with calcein-AM alone, with the fluorescence peak channel being 41 versus 315 and mean fluorescence at 47 versus 400, respectively (Fig. 8, left panel). Thus, the PTP opening can be followed in cell populations by fluorescence-activated cell sorter analysis of cells loaded with calcein-AM in the presence of Co^{2+} . Figure 8, right panel, indeed shows that 3 μ M BMAP-28 caused a remarkable attenuation of the calcein fluorescence, which was evident also under the microscope, where part of the cell population showed dim or no fluorescence (Fig. 7D). The addition of CsA largely prevented the loss of green fluorescence otherwise caused by BMAP-28, maintaining the fraction of fluorescent cells and the fluorescence intensity at values comparable to those of control cell populations. When treated with BMAP-28 in the presence of CsA, the cells were 87% fluorescent (peak channel, 38) and the control cell population exposed to CsA included 92% of fluorescent cells (peak channel, 39).

We next investigated whether PTP opening by BMAP-28 was followed by cytochrome *c* release in situ with the sensitive double-labeling protocol that was recently developed in one of our laboratories (30). The experimental results shown in Fig. 9, top and middle panels, show that after the addition of 3 to 6 μ M BMAP-28 the distribution of cytochrome *c* no longer matched that of the bc_1 complex, as shown by the time-dependent decrease of the localization index, which indicates that the distribution of cytochrome *c* is more diffuse than that of the bc_1 complex (see reference 30 for details). The PTP was at least partly involved in cytochrome *c* release because CsA delayed this process. Indeed, at 30 min CsA failed to affect cytochrome *c* release mediated by BMAP-28. However, CsA inhibited the

release in cells treated with 3 or 6 μ M BMAP-28 for 15 min, since the colocalization index (0, 97) was similar to the one observed in the control cell population (1, 01).

The release of cytochrome *c* at 15 min was accompanied by initiation of a cell death program, since cells pulsed with BMAP-28 and then cultured in peptide-free medium displayed DNA laddering already after 6 h, which further increased at 18 h, when extensive degradation prevented visualization of intact high-molecular-weight DNA fragments (Fig. 9, bottom panel).

DISCUSSION

In the past years, functions other than microbicidal activity have been ascribed to antimicrobial peptides (33). For instance, defensins (22) and magainins (29) are cytotoxic to normal or transformed mammalian cells. Some peptides can modulate cellular events involved in the inflammatory response such as syndecan expression (14), chemotaxis (17, 44), or chloride secretion (24). A hallmark of most antimicrobial peptides is a membrane-permeabilizing activity, which has also been investigated in mitochondria, mostly used as model targets. Antibacterial peptides from insects (melittin and cecropins) and from mammals (magainins) as well as artificial short cecropin A-melittin hybrids have been shown to affect mitochondrial coupling and respiration (11, 18). Finally, mastoparan, a peptide from the venom of *Vespa laevis*, has been shown to be a potent inducer of the PTP even in the absence of added Ca^{2+} (32). Our data add BMAP-28, a cathelicidin-derived peptide, to the number of mitochondrially active peptides and provide a novel mechanism for its cytotoxic activity, which appears to be mediated by early PTP opening and cytochrome *c* release.

To test this point, we have studied the effects of BMAP-28 on mitochondrial permeability and energy coupling in both

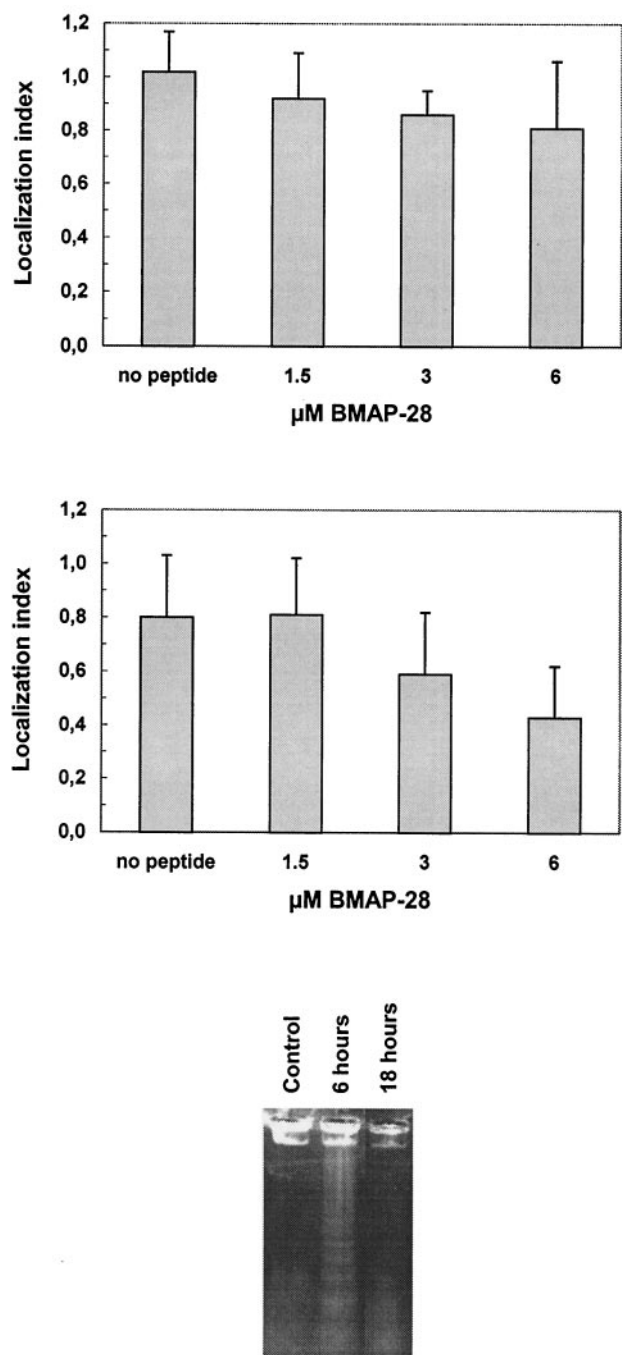


FIG. 9. BMAP-28 induces release of cytochrome *c* from mitochondria in situ and subsequent DNA fragmentation. U937 cells were incubated with the indicated peptide concentrations in PBS-5 mM glucose for 15 min (top panel) or 30 min (middle panel) and then fixed as detailed in Materials and Methods and reference 30. Cells were then spun onto slides for analysis with the confocal microscope. A localization index of 1 indicates that cytochrome *c* and the bc_1 complex have the same distribution, while an index lower than 1 means that the distribution of cytochrome *c* is more homogeneous than that of the bc_1 complex, i.e., that cytochrome *c* has diffused away from the mitochondria. The error bars refer to the SD of 25 individual cells for each condition. For further details, see reference 30. The bottom panel reports the analysis of DNA fragmentation in U937 cells pulsed with 3 μ M BMAP-28 for 15 min in PBS-glucose and then washed and resuspended in peptide-free culture medium at a cell density of 1×10^6 cells/ml. At 6 and 18 h, the overall cell number had decreased to 56 and

isolated mitochondria and intact cells. We have established that, besides plasma membrane permeabilization, BMAP-28 depolarizes mitochondria in situ, suggesting that mitochondrial dysfunction is the cause rather than the consequence of cell death and that mitochondrial depolarization is caused by opening of the PTP, as shown by its inhibition by CsA and potentiation by Ca^{2+} . Although the peptide mediates extracellular Ca^{2+} influx into the cells (34), mitochondrial depolarization was induced by BMAP-28 even without the synergistic effect of Ca^{2+} (Fig. 2), suggesting that the intracellular Ca^{2+} rise may not be the primary, or the only, cause of the $\Delta\Psi_m$ decrease. We would like to stress that these effects were observed in three BMAP-28-sensitive cell types (two tumor cell lines and activated normal lymphocytes), suggesting that this mitochondrial mechanism of cytotoxicity may be of general significance.

The effects of BMAP-28 on mitochondria in situ. Analysis of mitochondrial function in situ with fluorescent probes is not trivial, and a key issue is the interpretation of the observed fluorescence changes. We stress that in the present work we have carefully considered and experimentally ruled out the major potential sources of artifacts and misinterpretations. The four most troublesome aspects are the following. (i) Depending on the probe and its concentration, mitochondrial depolarization may be accompanied by a fluorescence decrease or increase (27), due to the variable contribution of fluorescence quenching by mitochondrial accumulation, which would subtract from the total cellular signal. We have found that in our experimental conditions the direction of the fluorescence change induced by BMAP-28 is the same as that of the protonophore FCCP (Fig. 1), whose depolarizing effects on mitochondria have been thoroughly characterized. This in turn allows us to conclude that the decrease of the red JC-1 fluorescence is indeed due to a mitochondrial depolarization, which is in line with previous observations (9, 12).

(ii) A second problem is that potentiometric probes are substrates of the multidrug resistance P glycoprotein, which like the PTP can be inhibited by CsA (6, 7). In accord with the literature (2), we have found that the multidrug-resistant P glycoprotein has a negligible activity in the U937 batch of cells that we are using, as shown by experiments with rhodamine 123 release. These results indicate that the effects of CsA on the JC-1 fluorescence changes induced by BMAP-28 are indeed due to PTP inhibition.

(iii) A third problem is that mitochondrial probe accumulation may be affected by variations of the plasma membrane potential (6, 7, 27). Although we have not formally investigated this possibility, which is remote with the slowly redistributing JC-1, we are confident that the changes that we observe are of mitochondrial origin because they are inhibited by CsA. Furthermore, independent evidence that BMAP-28 causes PTP opening was obtained from the experiments with trapped calcein, which does not undergo membrane potential-dependent redistribution and therefore is not affected by changes of the plasma membrane potential.

53% of the inoculum, respectively. Of these, 40% were viable for both incubation times (as measured by trypan blue exclusion). After 6 and 18 h, 4×10^5 cells were harvested and processed for analysis of DNA fragmentation as described in Materials and Methods.

(iv) Finally, mitochondrial depolarization may represent the physiological response of healthy mitochondria to an increased energy demand rather than a sign of mitochondrial dysfunction (6, 7). This is not the case for BMAP-28-dependent mitochondrial depolarization because this was prevented by the PTP inhibitor CsA but not by the F_1F_0 inhibitor oligomycin (not shown).

Thus, taken together our results conclusively demonstrate that BMAP-28 induces PTP opening in situ and suggest that this is due to a modulation of the PTP open time by the peptide. As discussed more in detail below, however, whether the in situ effects of BMAP-28 on the PTP are direct or indirect remains an open question.

Interactions of BMAP-28 with mitochondria and cells. We have documented that in isolated mouse liver mitochondria a CsA-sensitive mitochondrial permeability transition is caused by relatively low concentrations (below 1 μ M) of BMAP-28 but not of the truncated BMAP-28(1-18). At higher concentrations (above 2 μ M), the onset of mitochondrial permeabilization is faster while the sensitivity to CsA tends to disappear. This finding may suggest that at higher concentrations the peptide causes direct membrane permeabilization, which is consistent with a low but measurable permeabilizing activity of the truncated BMAP-28(1-18) peptide in isolated mitochondria. Yet, two very important points must be borne in mind. (i) With most PTP inducers, the sensitivity to CsA tends to disappear as the inducer concentration is raised (4); it is thus likely that the permeabilizing effects of BMAP-28 in the near-micromolar (cytotoxic) range are largely if not exclusively due to PTP opening rather than to a detergent-like effect. (ii) Although a permeability transition is detected in mitochondrial suspensions treated with peptide concentrations below 1 μ M, i.e., lower than the cytotoxic concentration, it is reasonable to assume that only a fraction of the peptide added to the cell suspension may gain access to the mitochondrial inner membrane. In any case, these results document that the mitochondrion is a functional target of the cytotoxic effect of BMAP-28. This may be either due to peptide targeting to the mitochondrial inner membrane, possibly through its hydrophobic C-terminal sequence, or to indirect effects, e.g., on intracellular Ca^{2+} homeostasis or on other yet unidentified signaling pathways to the mitochondrion. Although we currently have no elements to favor either hypothesis, we note that they are not mutually exclusive and may well reinforce one another. While the signaling role of Ca^{2+} to the PTP is out of the question, it is also true that more than one stimulus is often needed to tip the balance of the pore open-closed transitions towards the open state (6, 7).

Mechanism of BMAP-28 cytotoxicity. The early effects of BMAP-28 on mitochondria (mitochondrial depolarization due to PTP opening and cytochrome *c* release) suggest that these events are determinants of BMAP-28 toxicity. Release of cytochrome *c* from mitochondria in situ is consistent with a permeability change caused by BMAP-28 and suggests a mechanistic link with the lethal effect of the peptide in intact cells. This is also consistent with DNA fragmentation, which could be observed in cells pulsed with BMAP-28 for 15 min and then incubated in peptide-free culture medium. It should be stressed, however, that these experiments do not prove that cytochrome *c* release is occurring in the same cells undergoing

DNA degradation, an issue that can only be addressed when the response takes place in the whole cell population. Whether the DNA degradation is due to direct endonuclease activation through release of apoptosis-inducing factor (19, 38), to caspases activated by release of cytochrome *c* and possibly Smac-Diablo (13, 41), or to yet different mechanisms remains matter for future investigation. Our results should not be taken to imply that mitochondrial permeabilization through a permeability transition is the only mechanism through which BMAP-28 affects cell function. Indeed, BMAP-28 interaction with the plasma membrane causes an early rise of cytoplasmic Ca^{2+} (34), which may be an important additional factor generating intracellular signals that synergize with PTP opening in causing cell death.

ACKNOWLEDGMENTS

This work was supported by the MURST projects COFIN 2000 (R.G. and M.Z.), COFIN 2000-2001 (A.V.), and Bioenergetica e Trasporto di Membrana (P.B.) and by the Armenise-Harvard Foundation (P.B.). M.C.S. was supported by a postdoctoral fellowship from the University of Padua.

We are grateful to Marina Giunta (Istituto di Genetica, Policlinico Universitario di Udine) for assistance with epifluorescence microscopy.

REFERENCES

- Ankarcrona, M., J. M. Dypbukt, E. Bonfoco, B. Zhivotovsky, S. Orrenius, S. A. Lipton, and P. Nicotera. 1995. Glutamate-induced neuronal death: a succession of necrosis or apoptosis depending on mitochondrial function. *Neuron* **15**:961-973.
- Bailly, J. D., C. Muller, J. P. Jaffrezou, C. Demur, G. Gassar, C. Bordier, and G. Laurent. 1995. Lack of correlation between expression and function of P-glycoprotein in acute myeloid leukemia cell lines. *Leukemia* **9**:799-807.
- Bernardi, P., S. Vassanelli, P. Veronese, R. Colonna, I. Szabo, and M. Zoratti. 1992. Modulation of the mitochondrial permeability transition pore. Effects of protons and divalent cations. *J. Biol. Chem.* **267**:2934-2939.
- Bernardi, P. 1999. Mitochondrial transport of cations: channels, exchangers, and permeability transition. *Physiol. Rev.* **79**:1127-1155.
- Bernardi, P. 1992. Modulation of the mitochondrial cyclosporin A-sensitive permeability transition pore by the proton electrochemical gradient. Evidence that the pore can be opened by membrane depolarization. *J. Biol. Chem.* **267**:8334-8339.
- Bernardi, P., V. Petronilli, F. Di Lisa, and M. Forte. 2001. A mitochondrial perspective on cell death. *Trends Biochem. Sci.* **26**:112-117.
- Bernardi, P., L. Scorrano, R. Colonna, V. Petronilli, and F. Di Lisa. 1999. Mitochondria and cell death. Mechanistic aspects and methodological issues. *Eur. J. Biochem.* **264**:687-701.
- Brenner, G., and G. Kroemer. 2000. Apoptosis. Mitochondria—the death signal integrators. *Science* **289**:1150-1151.
- Cossarizza, A., M. Baccarani-Contri, G. Kalashnikova, and C. Franceschi. 1993. A new method for the cytofluorimetric analysis of mitochondrial membrane potential using the J-aggregate forming lipophilic cation 5,5',6,6'-tetrachloro-1,1',3,3'-tetraethylbenzimidazolcarbocyanine iodide (JC-1). *Biochem. Biophys. Res. Commun.* **197**:40-45.
- Crompton, M. 2000. Bax, Bid and the permeabilization of the mitochondrial outer membrane in apoptosis. *Curr. Opin. Cell Biol.* **12**:414-419.
- Diaz-Achirica, P., S. Prieto, J. Ubach, D. Andreu, E. Rial, and L. Rivas. 1994. Permeabilization of the mitochondrial inner membrane by short cecropin-A-melittin hybrid peptides. *Eur. J. Biochem.* **224**:257-263.
- Di Lisa, F., P. S. Blank, R. Colonna, G. Gambassi, H. S. Silverman, M. D. Stern, and R. G. Hansford. 1995. Mitochondrial membrane potential in single living adult rat cardiac myocytes exposed to anoxia or metabolic inhibition. *J. Physiol. (London)* **486**:1-13.
- Du, C., M. Fang, Y. Li, L. Li, and X. Wang. 2000. Smac, a mitochondrial protein that promotes cytochrome *c*-dependent caspase activation by eliminating IAP inhibition. *Cell* **102**:33-42.
- Gallo, R., M. Ono, T. Povsic, C. Page, E. Eriksson, M. Klagsbrun, and M. Bernfield. 1994. Syndecans, cell surface heparan sulfate proteoglycans, are induced by a proline-rich antimicrobial peptide from wounds. *Proc. Natl. Acad. Sci. USA* **91**:11035-11039.
- Green, D. R., and J. C. Reed. 1998. Mitochondria and apoptosis. *Science* **281**:1309-1312.
- Helmerhorst, E. J., P. Breeuwer, W. van't Hof, E. Walgreen-Weterings, L. C. Oomen, E. Veerman, A. Amerongen, and T. Abee. 1999. The cellular target

- of histatin 5 on *Candida albicans* is the energized mitochondrion. *J. Biol. Chem.* **274**:7286–7291.
17. Huang, H., C. R. Ross, and F. Blecha. 1997. Chemoattractant properties of PR39, a neutrophil antibacterial peptide. *J. Leukoc. Biol.* **61**:624–629.
 18. Hugosson, M., D. Andreu, H. G. Boman, and E. Glaser. 1994. Antibacterial peptides and mitochondrial presequences affect mitochondrial coupling, respiration and protein import. *Eur. J. Biochem.* **223**:1027–1033.
 19. Joza, N., S. A. Susin, E. Daugas, W. L. Stanford, S. K. Cho, C. Y. Li, T. Sasaki, A. J. Elia, H. Y. Cheng, L. Ravagnan, K. F. Ferri, N. Zamzami, A. Wakeham, R. Hakem, H. Yoshida, Y. Y. Kong, T. W. Mak, J. C. Zuniga-Pflucker, G. Kroemer, and J. M. Penninger. 2001. Essential role of the mitochondrial apoptosis-inducing factor in programmed cell death. *Nature* **410**:549–552.
 20. Krajewski, S., M. Krajewska, L. M. Ellerby, K. Welsh, Z. Xie, Q. L. Deveraux, G. S. Salvesen, D. E. Bredesen, R. E. Rosenthal, G. Fiskum, and J. C. Reed. 1999. Release of caspase-9 from mitochondria during neuronal apoptosis and cerebral ischemia. *Proc. Natl. Acad. Sci. USA* **96**:5752–5757.
 21. Kroemer, G., B. Dallaporta, and M. Resche-Rigon. 1998. The mitochondrial death/life regulator in apoptosis and necrosis. *Annu. Rev. Physiol.* **60**:619–642.
 22. Lehrer, R. I., A. K. Lichtenstein, and T. Ganz. 1993. Defensins: antimicrobial and cytotoxic peptides of mammalian cells. *Annu. Rev. Immunol.* **11**:105–128.
 23. Lemasters, J. J., T. Qian, C. A. Bradham, D. A. Brenner, W. E. Cascio, L. C. Trost, Y. Nishimura, A. L. Nieminen, and B. Herman. 1999. Mitochondrial dysfunction in the pathogenesis of necrotic and apoptotic cell death. *J. Bioenerg. Biomembr.* **31**:305–319.
 24. Lencer, W. I., G. Cheung, G. R. Strohmeier, M. G. Currie, A. J. Ouellette, M. E. Selsted, and J. L. Madara. 1997. Induction of epithelial chloride secretion by channel-forming cryptidins 2 and 3. *Proc. Natl. Acad. Sci. USA* **94**:8585–8589.
 25. Lichtenstein, A. 1991. Mechanism of mammalian cell lysis mediated by peptide defensins. Evidence for an initial alteration of the plasma membrane. *J. Clin. Investig.* **88**:93–100.
 26. Lichtenstein, A. K., T. Ganz, T. Nguyen, M. Selsted, and R. I. Lehrer. 1988. Mechanism of target cytolysis by peptide defensins. Target cell metabolic activities, possibly involving endocytosis, are crucial for expression of cytotoxicity. *J. Immunol.* **140**:2686–2694.
 27. Nicholls, D. G., and M. W. Ward. 2000. Mitochondrial membrane potential and neuronal glutamate excitotoxicity: mortality and millivolts. *Trends Neurosci.* **23**:166–174.
 28. Nicolli, A., E. Basso, V. Petronilli, R. M. Wenger, and P. Bernardi. 1996. Interactions of cyclophilin with the mitochondrial inner membrane and regulation of the permeability transition pore, a cyclosporin A-sensitive channel. *J. Biol. Chem.* **271**:2185–2192.
 29. Ohsaki, Y., A. F. Gazdar, H. C. Chen, and B. Johnson. 1992. Antitumor activity of magainin analogues against human lung cancer cell lines. *Cancer Res.* **52**:3534–3538.
 30. Petronilli, V., D. Penzo, L. Scorrano, P. Bernardi, and F. Di Lisa. 2000. The mitochondrial permeability transition, release of cytochrome *c* and cell death. Correlation with the duration of pore openings *in situ*. *J. Biol. Chem.* **276**:12030–12034.
 31. Petronilli, V., G. Miotto, M. Canton, M. Brini, R. Colonna, P. Bernardi, and F. Di Lisa. 1999. Transient and long-lasting openings of the mitochondrial permeability transition pore can be monitored directly in intact cells by changes in mitochondrial calcein fluorescence. *Biophys. J.* **76**:725–734.
 32. Pfeiffer, D., T. I. Gudz, S. A. Novgorodov, and W. Erdhal. 1994. The peptide mastoparan is a potent facilitator of the mitochondrial permeability transition. *J. Biol. Chem.* **270**:4923–4932.
 33. Risso, A. 2000. Leukocyte antimicrobial peptides: multifunctional effector molecules of innate immunity. *J. Leukoc. Biol.* **68**:785–792.
 34. Risso, A., M. Zanetti, and R. Gennaro. 1998. Cytotoxicity and apoptosis mediated by two peptides of innate immunity. *Cell. Immunol.* **189**:107–115.
 35. Shimizu, S., M. Narita, and Y. Tsujimoto. 1999. Bcl-2 family proteins regulate the release of apoptogenic cytochrome *c* by the mitochondrial channel VDAC. *Nature* **399**:483–487.
 36. Skerlavaj, B., R. Gennaro, L. Bagella, L. Merluzzi, A. Risso, and M. Zanetti. 1996. Biological characterization of two novel cathelicidin-derived peptides and identification of structural requirements for their antimicrobial and cell lytic activities. *J. Biol. Chem.* **271**:28375–28381.
 37. Susin, S. A., H. K. Lorenzo, N. Zamzami, I. Marzo, K. Brenner, N. Larochette, M. C. Prevost, P. M. Alzari, and G. Kroemer. 1999. Mitochondrial release of caspase-2 and -9 during the apoptotic process. *J. Exp. Med.* **189**:381–394.
 38. Susin, S. A., H. K. Lorenzo, N. Zamzami, I. Marzo, B. E. Snow, G. M. Brothers, J. Mangion, E. Jacotot, P. Costantini, M. Loeffler, N. Larochette, D. R. Goodlett, R. Aebersold, D. P. Siderovski, J. M. Penninger, and G. Kroemer. 1999. Molecular characterization of mitochondrial apoptosis-inducing factor. *Nature* **397**:441–446.
 39. Susin, S. A., N. Zamzami, M. Castedo, E. Daugas, H. G. Wang, S. Geley, F. Fassy, J. Reed, and G. Kroemer. 1997. The central executioner of apoptosis: multiple connections between protease activation and mitochondria in Fas/APO-1/CD95- and ceramide-induced apoptosis. *J. Exp. Med.* **186**:25–37.
 40. Vande Velde, C., J. Cizeau, D. Dubik, J. Alimonti, T. Brown, S. Israels, R. Hakem, and A. H. Greenberg. 2000. BNIP3 and genetic control of necrosis-like cell death through the mitochondrial permeability transition pore. *Mol. Cell. Biol.* **20**:5454–5468.
 41. Verhagen, A. M., G. Ekert, M. Pakusch, J. Silke, L. M. Connolly, G. E. Reid, R. L. Moritz, R. J. Simpson, and D. L. Vaux. 2000. Identification of DIA-BLO, a mammalian protein that promotes apoptosis by binding to and antagonizing IAP proteins. *Cell* **102**:43–53.
 42. Vianello, A., F. Macri, E. Braidot, and E. N. Mokhova. 1995. Effect of 6-ketocholestanol on FCCP- and DNP-induced uncoupling in plant mitochondria. *FEBS Lett.* **365**:7–9.
 43. Weaver, J. L., P. S. Pine, A. Aszalos, P. V. Schoenlein, S. J. Currier, R. Padmanabhan, and M. M. Gottesman. 1991. Laser scanning and confocal microscopy of daunorubicin, doxorubicin, and rhodamine 123 in multidrug-resistant cells. *Exp. Cell Res.* **196**:323–329.
 44. Yang, D., O. Chertov, S. N. Bykovskaia, Q. Chen, M. J. Buffo, J. Shogan, M. Anderson, J. M. Schroeder, J. M. Wang, O. M. Z. Howard, and J. J. Oppenheim. 1999. Beta-defensins: linking innate and adaptive immunity through dendritic and T cell CCR6. *Science* **286**:525–528.
 45. Zanetti, M., R. Gennaro, and D. Romeo. 1995. Cathelicidins: a novel protein family with a common proregion and a variable C-terminal antimicrobial domain. *FEBS Lett.* **374**:1–5.
 46. Zanotti, A., and G. F. Azzone. 1980. Safranin as membrane potential probe in rat liver mitochondria. *Arch. Biochem. Biophys.* **201**:255–265.